Mathematical Medicine and Biology (2018) **35**, 387–407
doi: 10.1093/imammb/dqx009
Advance Access publication on 7 August 2017

Analysing the dynamics of a model for alopecia areata as an autoimmune disorder of hair follicle cycling

ATANASKA DOBREVA[†]
Department of Mathematics, 208 Love Building, 1017 Academic Way, Florida State University, Tallahassee, FL 32306, USA
[†]Corresponding author. Email: adobreva@math.fsu.edu

RALF PAUS
Centre for Dermatology Research, University of Manchester, and NIHR Manchester Biomedical Research Centre, Manchester, UK

AND

N. G. COGAN
Department of Mathematics, 208 Love Building, 1017 Academic Way, Florida State University, Tallahassee, FL 32306, USA

[Received on 25 August 2016; revised on 12 June 2017; accepted on 26 June 2017]

Alopecia areata (AA) is a $CD8^+$ T cell-dependent autoimmune disease that disrupts the constantly repeating cyclic transformations of hair follicles (HFs). Among the three main HF cycle stages—growth (anagen), regression (catagen) and relative quiescence (telogen)—only anagen HFs are attacked and thereby forced to prematurely enter into catagen, thus shortening active hair growth substantially. After having previously modelled the dynamics of immune system components critically involved in the disease development (Dobreva *et al.*, 2015), we here present a mathematical model for AA which incorporates HF cycling and illustrates the anagen phase interruption in AA resulting from an inflammatory autoimmune response against HFs. The model couples a system describing the dynamics of autoreactive immune cells with equations modelling the hair cycle. We illustrate states of health, disease and treatment as well as transitions between them. In addition, we perform parameter sensitivity analysis to assess how different processes, such as proliferation, apoptosis and input from stem cells, impact anagen duration in healthy versus AA-affected HFs. The proposed model may help in evaluating the effectiveness of existing treatments and identifying new potential therapeutic targets.

Keywords: alopecia areata; hair cycle disruption; hair loss; autoimmunity.

1. Introduction

Alopecia areata (AA) is one of the most common autoimmune diseases and causes highly characteristic patterns of hair loss (Gilhar *et al.*, 2012). A key feature of AA is that it disrupts the natural, constantly repeating cycle of hair follicles (HFs) which has three main stages: anagen (growth), catagen (regression) and relative quiescence (telogen) (Schneider *et al.*, 2009; Geyfman *et al.*, 2014; Oh *et al.*, 2016). The characteristic perifollicular inflammatory infiltrate in AA, without which the disease does not occur, attacks exclusively anagen HFs and significantly shortens the length of the growth phase, while the duration of catagen and telogen presumably remain largely unaffected. In addition, the autoimmune

infiltrate damages anagen HFs and thus causes major HF dystrophy so that anagen HFs can no longer retain their hair shaft, which is subsequently lost, shed, or breaks off (Gilhar *et al.*, 2012; McElwee *et al.*, 2013).

However, AA is not only a disorder of HF cycling in a dual sense in that it affects essentially only one of three hair cycle phases and then disrupts HF integrity and cycling as such. Like so many other autoimmune diseases (Rose & Mackay, 2013), in many affected patients, it also shows a dynamic, chronic course of clinical disease relapses and remissions, often with long stretches of pseudo-dormancy, that can generate an approximatively cyclic disease biography over the lifetime of some AA patients (McDonagh & Messenger, 2001; D'Ovidio, 2014). Thus, we are faced with a disorder that is temporally restricted (i.e. to one window in the cyclic transformations of the HF), but persists beyond this temporal restriction; disrupts a chronobiological, cyclic organ remodelling system (the HF cycle) (Hardman *et al.*, 2015; Oh *et al.*, 2016); and typically is cyclic in its waxing and waning of perifollicular inflammatory events associated with distinct clinical phenomena (hair loss and regrowth). By its very nature, such a disorder is therefore uniquely suited for, and should profit from, the application of computational and systems biology tools (Waterman, 1995; Pevzner, 2000; Westerhoff *et al.*, 2007; Al-Nuaimi *et al.*, 2010), for example for drug design purposes (Westerhoff *et al.*, 2007, 2015), and may serve as a model disorder for other, pathobiologically related, yet less easily accessible and more difficult to assess autoimmune diseases.

Experimental evidence has demonstrated that critical players involved in the development of AA are autoreactive $CD8^+$ T-cells/$NKG2D^+$ cells and the pro-inflammatory cytokine interferon-γ (IFN-γ), along with help from $CD4^+$ T-cells (Ito *et al.*, 2008; Petukhova *et al.*, 2010; Gilhar *et al.*, 2012, 2013, 2016; McElwee *et al.*, 2013; Ito & Tokura, 2014; Xing *et al.*, 2014; Guo *et al.*, 2015). Perifollicular mast cells may play an additional, potentially important disease-modulatory role in AA by impacting on autoreactive $CD8^+$ T-cells (Bertolini *et al.*, 2014).

Moreover, AA only occurs when the physiological immune privilege (IP) of the HF is lost (Paus *et al.*, 2005). In this context, it has been shown that locally generated immunosuppressive agents, such as transforming growth factor-β (TGF-β1 and 2), alpha-melanocyte-stimulating hormone (α-MSH), calcitonin gene-related peptide and vasoactive intestinal peptide (VIP) all serve as important guardians of HF IP as they inhibit accumulation and/or activation of autoreactive lymphocytes and are capable of down-regulating excessive, ectopic expression of HF autoantigen-presenting MHC class I and class II molecules (Ito *et al.*, 2004; Paus *et al.*, 2005, 2008; Kinori *et al.*, 2012; McElwee *et al.*, 2013; Bertolini *et al.*, 2016). As recently shown for VIP receptors, the HF sensitivity to stimulation with these endogenous immunoinhibitory neuropeptides may be reduced in AA patients, constitutively or in response to the inflammatory infiltrate, thus rendering affected HFs and likely their immediate neighbours more susceptible to IP collapse (Bertolini *et al.*, 2016).

We previously proposed a mathematical model which captures interactions between immune system components and HFs and used it to simulate and distinguish three states of a small cluster of homogeneous HFs: healthy, diseased and treatment (Dobreva *et al.*, 2015). In order to focus on understanding the complex temporal dynamics of immune cells and signals in AA pathobiology, for pragmatic reasons, we assumed that HF are in the anagen phase, so we did not figure transition through the hair cycle stages into our equations. By tracking only the dynamics of immune components, we were able to accurately predict that a small, circumscript cluster of HFs develops the disease if and when the populations of autoreactive lymphocytes become sufficiently large (Dobreva *et al.*, 2015).

In the current article, instead, we relax the assumption of anagen-only HFs and allow cycling, so as to develop an optimized, more complex and *in vivo*-like model that tracks the dynamics of immune components as well as the dynamics of HF cycling, leaning in part on an earlier mathematical model of

human HF cycling (Al-Nuaimi *et al.*, 2012). In this way, we obtain a temporal mathematical model for AA that can exhibit hair cycle disruption in response to an autoimmune reaction directed against HFs. In addition, in the current, advanced model, we apply parameter sensitivity analysis to determine which processes exert the greatest impact in relation to the duration of anagen in healthy versus AA-affected HFs. With the sensitivity analysis, we focus on explaining how different processes reflected in the model influence the growth phase since AA is known to disrupt anagen, but does not seem to interfere with catagen and telogen (Gilhar *et al.*, 2012; McElwee *et al.*, 2013).

Note that while we recognize that telogen represents only seemingly, but not in fact, a 'resting' stage (Geyfman *et al.*, 2012, 2014), we hold that this is irrelevant for the purpose of the current discussion, since what matters in the current context is that telogen HFs appear to be protected from an attack by inflammatory cells in AA, while anagen HFs are highly susceptible to sustain damage from it (McDonagh & Messenger, 2001; Gilhar *et al.*, 2013; Ito & Tokura, 2014; Gilhar *et al.*, 2016).

2. Model description

2.1 *Model of the hair cycle*

Substantial amount of modelling has been done for hair cycle dynamics as reviewed by Al-Nuaimi *et al.* (2012), Bernard (2012), Baker & Murray (2012) and Murray *et al.* (2012). Different approaches have been utilized, such as bistability assumptions (Bernard, 2012; Al-Nuaimi *et al.*, 2012), cellular automaton models (Halloy *et al.*, 2000, 2002; Plikus *et al.*, 2011), systems of ordinary and stochastic differential equations reflecting dynamics at the molecular level (Murray *et al.*, 2012) and a system of ordinary differential equations describing dynamics at the cell population level (Al-Nuaimi *et al.*, 2012).

Here we focus on reviewing in more detail the model proposed in Al-Nuaimi *et al.* (2012), which is of particular relevance for the current study, as in the following sections we work to connect the Al-Nuaimi *et al.* model with a system that captures the behaviour of autoreactive immune cells. The cycle dynamics of a healthy HF are modelled with a system of ordinary differential equations (2.1)–(2.5) that reflect interactions between two compartments, matrix keratinocytes (MKs) and dermal papilla (DP). A schematic representation of the model is shown in Fig. 1. MKs are the most rapidly proliferating cells of the human HF epithelium that produce the hair fibre (Purba *et al.*, 2016), and the DP, the mesenchymal 'command center' of the HF, exerts control over the number of MKs due to the secretion of growth factors/morphogens it supplies (or does not supply) to MKs, thereby controlling MK proliferation (Van Scott and Ekel, 1958; Paus and Foitzik , 2004; Ohyama *et al.*, 2010; Morgan, 2014). The model variables are as follows (Al-Nuaimi *et al.*, 2012):

- ξ: population of MKs
- η_1: signalling molecule produced by MKs
- η_2: signalling molecule produced in the DP
- z_1: regulatory molecule affecting MKs directly
- z_2: regulatory molecule affecting MKs indirectly.

As presented in Al-Nuaimi *et al.* (2012), ξ is the number of MKs re-scaled by a factor of 100. During the hair cycle, the number of MKs ranges from 0 to about 600 cells: In telogen, there are approximately 30 MKs; in anagen their number increases to about 600, and during catagen the number of MKs decreases to

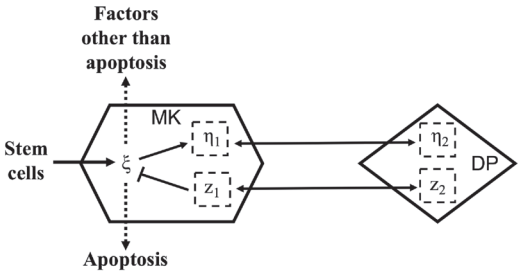

FIG. 1. Schematic representation of hair cycle model. The MK population (ξ) increases through proliferation and stem cell input, and declines due to apoptosis and other factors. DP cells also influence the number of MKs. Communication between MKs and DP cells is mediated by signalling molecules (η_1, η_2) and regulatory molecules (z_1, z_2).

0 (Al-Nuaimi *et al.*, 2012). The η and z variables represent molecular concentrations (Al-Nuaimi *et al.*, 2012).

The regulatory and signalling molecules permeate between the two compartments and into the surroundings. The MK population grows through proliferation ($p_1\xi$) and stem cell input (α) and declines due to apoptosis ($-p_4\xi$) and other factors such as differentiation ($-\beta\xi$). MK population increase is saturating with a half-saturation constant of p_2, and the regulatory molecule z_1 inhibits proliferation of MKs $\left(\frac{p_1\xi}{(p_2+\xi)(p_3+C_{prol}z_1)}\right)$ (Al-Nuaimi *et al.*, 2012). MK apoptosis is subject to feedforward inhibition whose strength is modulated by the parameter k $\left(-\frac{p_4\xi}{p_5^k+\xi^k}\right)$. Putting these together, the following equations govern the dynamics of the HF (Al-Nuaimi *et al.*, 2012).

$$\frac{d\xi}{dt} = \frac{p_1\xi}{(p_2+\xi)\left(p_3+C_{prol}z_1\right)} - \frac{p_4\xi}{p_5^k+\xi^k} + \alpha - \beta\xi \tag{2.1}$$

$$\frac{d\eta_1}{dt} = c_1\xi + D_\eta(\eta_2 - 2\eta_1) \tag{2.2}$$

$$\frac{d\eta_2}{dt} = D_\eta(\eta_1 - 2\eta_2) \tag{2.3}$$

$$\frac{dz_1}{dt} = D_z(z_2 - 2z_1) \tag{2.4}$$

$$\frac{dz_2}{dt} = c_2\eta_2 + D_z(z_1 - 2z_2) \tag{2.5}$$

The model exhibits relaxation oscillations, which are interpreted as shown in Fig. 2: the long upper state corresponds to anagen, the rapid transition corresponds to catagen, and the lower short state corresponds to telogen. Results from analysing the model show that perturbations to the parameter controlling MK apoptosis, p_4, lead to AA profile marked by shortened anagen stage (Al-Nuaimi *et al.*, 2012). However, no explanation is provided for the perturbation regimes in the context of activities of cytokines and leukocytes.

In Section 2.3 we introduce a change to the Al-Nuaimi *et al.* model. Specifically, we modify the term for MK apoptosis in order to link this process to the dynamics of key immune components that drive AA

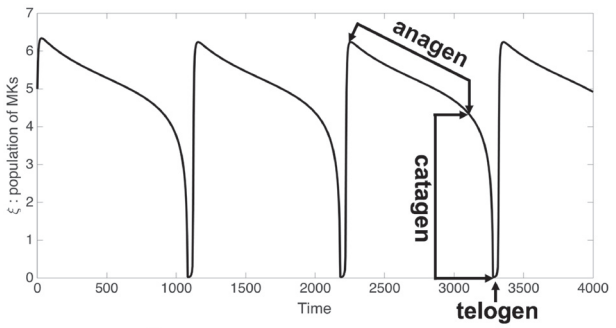

FIG. 2. Simulation of the hair cycle model of Al-Nuaimi *et al.* (2012). Interpretation of relaxation oscillations: The long upper state is anagen, the rapid transition is catagen and the short lower state is telogen. Dynamics are shown to develop on a physiological time scale.

pathobiology (Gilhar *et al.*, 2012). The purpose for making the change is so that one can clearly see how the hair cycle gets affected as the behaviour of autoreactive lymphocytes evolves over time.

2.2 *Model for immune system components*

We previously modelled the development of AA in a small cluster of homogeneous HFs with a dynamical system that reflects interactions between immune system components and HF IP guardians (HF IPG). Equations (2.6)–(2.7) comprise the reduction of the full model where x denotes the scaled population size of $CD8^+$ T-cells/$NKG2D^+$ cells, and y is the scaled number of $CD4^+$ T-cells. The autoreactive lymphocyte populations increase as cells migrate, get activated and proliferate. Activation and proliferation of lymphocytes is stimulated by IFN-γ. On the other hand, migration, activation and proliferation of $CD4^+$ and $CD8^+$ T-cells/$NKG2D^+$ cells are inhibited by HF IPG. The lymphocyte populations decrease due to natural as well as concentration-dependent cell death (Dobreva *et al.*, 2015). After a time scale argument to reduce the system, we obtained:

$$\frac{dx}{d\tau} = \frac{v(x+y)}{(1+s)\,(a+y+x)} + \frac{lxy}{(1+s)} - x - x^2 \tag{2.6}$$

$$\frac{dy}{d\tau} = \frac{b(x+y)}{(1+s)} + \frac{wy}{(1+s)} - y - y^2. \tag{2.7}$$

The model is able to capture three states: healthy, diseased and treatment (Fig. 3). In the healthy state, autoreactive immune cell populations decrease to zero with time. The diseased state develops in response to increased secretion of IFN-γ and involves large accumulation of immune cells in the small cluster of HFs. The treatment state simulation illustrates that high amount of strong HF IPG brings the lymphocyte populations to very low levels which leads to disease suppression. Analysing the model through Partial Rank Correlation Coefficient (PRCC) sensitivity analysis shows that IFN-γ and HF IPG are the most important processes in the development of AA (Dobreva *et al.*, 2015). These findings are biologically plausible as they are in accordance with the IP collapse model of AA pathogenesis of Paus *et al.* (1993), which has become widely accepted (Gilhar *et al.*, 2012; McElwee *et al.*, 2013; Ito & Tokura, 2014; Islam *et al.*, 2015).

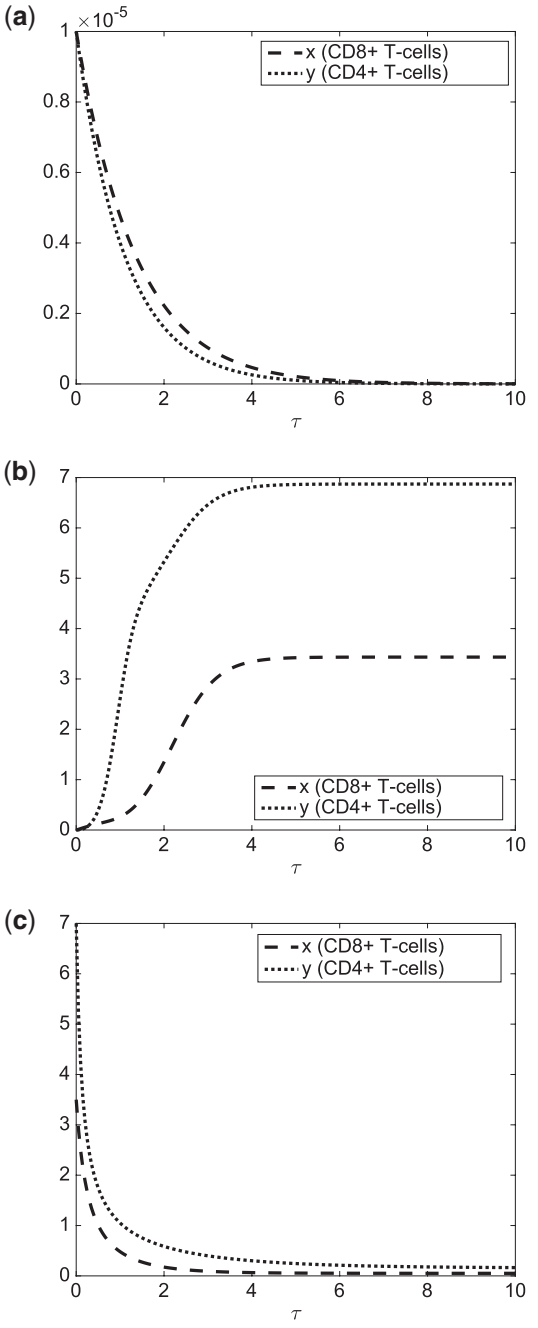

FIG. 3. Illustrative simulations of model for immune system components. The system captures three states: healthy, diseased and treatment. x-scaled $CD8^+$ T-cell/$NKG2D^+$ cell population size, y-scaled $CD4^+$ T-cell population size. AA, alopecia areata; HF IPG, hair follicle IP guardians. (a) Healthy state. Immune cell levels go to zero with time. (b) Diseased state. High IFN-γ level leads to disease. (c) Treatment state. Large amount of strong HF IPG suppresses AA.

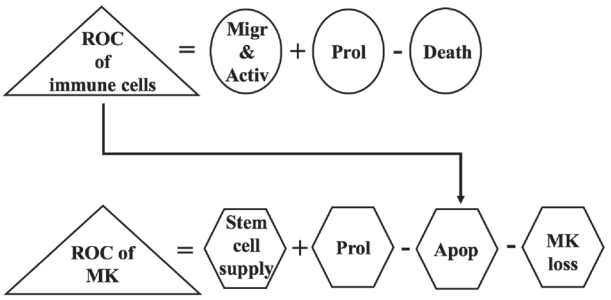

FIG. 4. Schematic representation of composite model. Autoreactive immune cells output feeds into the apoptosis term of the model for the hair cycle. When lymphocytes reach sufficiently high levels to cause disease, they contribute to premature apoptosis of MKs at an accelerated rate. MK, matrix keratinocyte; ROC, rate of change; Migr, migration; Activ, activation; Prol, proliferation; Apop, apoptosis.

We recognize that there are other immunocyte populations, such as mast cells, regulatory T-cells and NK cells, which may also have important involvement in AA pathobiology; however, these immune cells have been shown to play secondary roles (Gilhar *et al.*, 2012, 2013; McElwee *et al.*, 2013; Bertolini *et al.*, 2014). So, for the sake of keeping the immune components model simpler to work with and investigate, we refrain from including mast cells, regulatory T-cells and NK cells and leave the exploration of their AA-relevant dynamics to future studies.

2.3 *Composite model*

In the hair cycle model (2.1)–(2.5), parameter p_4 reflects the normal process of apoptosis that MKs go through during catagen. The autoimmune response in AA amplifies MK apoptosis, which promotes HF damage (causes dystrophic anagen) and abrogates anagen by prematurely inducing apoptosis-driven HF regression (catagen). Experimental studies have shown that autoreactive $CD4^+$ and $CD8^+$ T-cells/$NKG2D^+$ cells infiltrate the hair bulbs of diseased follicles and destroy MKs through cytotoxic activities, during which IFN-γ likely operates as the key cytokine (Xing *et al.*, 2014; McElwee *et al.*, 2013; Petukhova *et al.*, 2010; Gilhar *et al.*, 2012, 2013, 2016; Ito *et al.*, 2008; Ito & Tokura, 2014; Guo *et al.*, 2015). In particular, $CD8^+$ T-cells/$NKG2D^+$ cells, likely in concert with other immunocytes such as $CD4^+$ T cells, mast cells and NK cells, cause MKs to undergo premature and accelerated apoptosis which leads to disruption and early termination of both hair shaft formation and the anagen phase (Gilhar *et al.*, 2012; Ito, 2013; Bertolini *et al.*, 2014; Islam *et al.*, 2015).

To connect the equations for immune components with the system for MK dynamics and capture the influence of autoreactive lymphocytes, we introduce a function of $CD8^+$ T-cells/$NKG2D^+$ cells (x) and $CD4^+$ T-cells (y), $f(x, y)$, in the term which models MK apoptosis $\left(-\frac{f(x,y)p_4\xi}{p_5^k+\xi^k}\right)$. According to some experimental evidence, a cytotoxic T-cell is capable of inducing apoptosis, in a serial manner, in about 16 target cells per day (Halle *et al.*, 2016). Based on this estimate, we found it suitable to assume that f is a linear function of x and y, $f(x, y) = \lambda(x + y) + 1$. Note that for a healthy HF, we have $f(0, 0) = 1$.

Figure 4 shows a schematic representation of the composite model which comprises the following system of equations.

Immune components sub-model

$$\frac{dx}{dt} = \frac{v(x+y)}{(1+s)(a+y+x)} + \frac{lxy}{(1+s)} - x - x^2 \tag{2.8}$$

$$\frac{dy}{dt} = \frac{b(x+y)}{(1+s)} + \frac{wy}{(1+s)} - y - y^2 \tag{2.9}$$

Hair cycle sub-model

$$f(x,y) = \lambda(x+y) + 1 \tag{2.10}$$

$$\frac{d\xi}{dt} = \frac{p_1\xi}{(p_2+\xi)\left(p_3 + C_{prol}z_1\right)} - \frac{\boxed{f(x,y)}\,p_4\xi}{p_5^k + \xi^k} + \alpha - \beta\xi \tag{2.11}$$

$$\frac{d\eta_1}{dt} = c_1\xi + D_\eta(\eta_2 - 2\eta_1) \tag{2.12}$$

$$\frac{d\eta_2}{dt} = D_\eta(\eta_1 - 2\eta_2) \tag{2.13}$$

$$\frac{dz_1}{dt} = D_z(z_2 - 2z_1) \tag{2.14}$$

$$\frac{dz_2}{dt} = c_2\eta_2 + D_z(z_1 - 2z_2) \tag{2.15}$$

Note that the time scales for the physiological processes in each sub-model are quite different since, on average, the hair cycle lasts on the order of two to five years while the autoimmune dynamics develop on the order of fifty to a hundred days (Gilhar *et al.*, 1998; Al-Nuaimi *et al.*, 2012; Alli *et al.*, 2012; Gilhar *et al.*, 2012). To connect the two sub-models in a consistent time scale, we scale the immune components system by a factor of $\frac{1}{20}$. This is equivalent on a scale which is compatible with that described in our previous model (Dobreva *et al.*, 2015).

3. Analysis

We explore the behaviour of the composite model, described in Section 2.3, through simulation scenarios and also apply parameter sensitivity analysis to assess the importance of processes involved.

3.1 *Simulations*

We simulate the composite model in Matlab using a Runge-Kutta method of order 5. At each time step, the equations for $CD8^+$ T-cells (x) and $CD4^+$ T-cells (y) are solved first, and the output feeds into the apoptosis term of the equation for MKs through the function $f(x,y) = \lambda(x+y)+1$. The composite model parameters and their nominal levels are given in Table 1. We generate simulation scenarios by changing the parameter regime for the immune system components sub-model (parameters s to w). The scenarios we explore are as follows:

- Healthy state
- Diseased state
- Treatment state
- Transition from healthy state to diseased state

TABLE 1 *Nominal values of parameters in composite model*

Parameter	Nominal value	Biological significance
p_1	0.48	Proliferation of MKs
p_2	0.1	Half-saturation constant for MK population increase
p_3	0.1	Inhibition of MK proliferation associated with regulatory molecules
p_4	0.5	Apoptosis of MKs
p_5	0.32	Feedforward inhibition of apoptosis
C_{prol}	0.1	Inhibition of MK proliferation associated with regulatory molecules
α	0.1	Stem cell input to the MK population
β	0.1	Loss of MKs due to factors other than apoptosis
k	2.0385	Feedforward inhibition of MK apoptosis
c_1	1	Signalling molecule production
c_2	1	Regulatory molecule production
D_η	0.5	Permeation constant of signalling molecules
D_z	0.1	Permeation constant of regulatory molecules
λ	0.005	Impact of immune cells output on MK apoptosis
s	0.00034	Synthesis and strength of HF IP guardians
v	0.32	Migration, activation and loss of lymphocytes
l	0.6319	Proliferation and loss of lymphocytes
a	2.381	Synthesis of IFN-γ, loss of lymphocytes, half-saturation level of lymphocyte activation signals
b	0.000525	Synthesis of IFN-γ, migration, activation and loss of lymphocytes
w	0.0837	Ratio of proliferation rate to degradation rate of lymphocytes

*All parameters are dimensionless.

TABLE 2 *Healthy state, diseased state and state of treatment: Values of parameters for equations of immune components*

Parameter	Healthy state	Diseased state	State of treatment
s	0.00034	0.00034	5.10
v	0.32	0.32	0.32
l	0.6319	0.6319	0.6319
a	2.381	0.0002381	0.0002381
b	0.000525	5.25	5.25
w	0.0837	0.0837	0.0837

- Transition from diseased state to treatment state
- Transition from healthy state to diseased state to treatment state.

Healthy state: For the healthy state simulation all parameters are set to their nominal values listed in the second column of Table 2, and we use $x = 10^{-5}$ and $y = 10^{-5}$ as initial conditions to introduce negligible

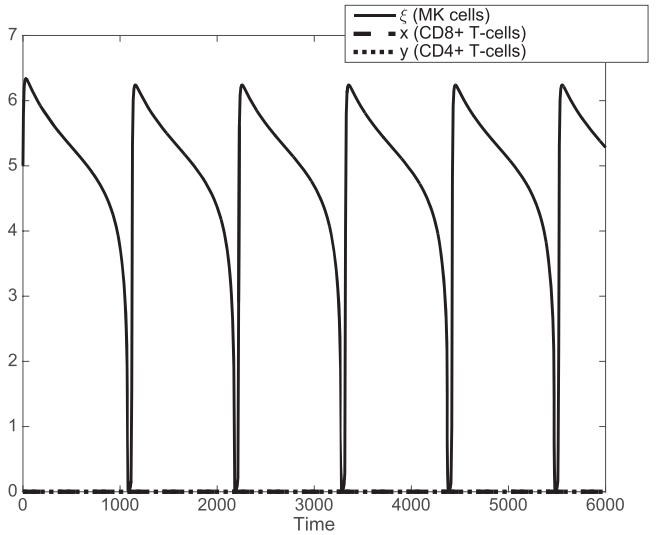

FIG. 5. Healthy state: Normal hair cycle. Autoreactive lymphocyte populations go to zero with time.

initial amount of autoreactive $CD8^+$ and $CD4^+$ T-cells to the system. The results in Fig. 5 show that over time the levels of autoreactive lymphocytes are brought down to zero, and the length of anagen is unaffected.

Diseased state: The third column of Table 2 provides the diseased state parameter regime: a and b have larger values to reflect an increase in IFN-γ, and all remaining parameters are at their nominal values. The initial conditions again are $x = 10^{-5}$ and $y = 10^{-5}$. In Fig. 6, we see that when IFN-γ is abnormally elevated, this leads to very large populations of $CD8^+$ and $CD4^+$ T-cells which bring about premature apoptosis of MKs and significantly shortened anagen phase.

Treatment state: The treatment state regime is given in the fourth column of Table 2: Parameters a and b are kept at their diseased state level; the larger value of s reflects increased amount and inhibitory ability of HF IP guardians, and all other parameters remain at nominal level. As initial conditions in this case, we use $x = 3.5$ and $y = 7$, the levels that $CD8^+$ and $CD4^+$ T-cells reach when a HF is diseased. The results in Fig. 7 show that sufficiently high amount of potent IP guardians causes the lymphocyte populations to decline to negligible levels at which AA is suppressed and the normal duration of anagen is restored.

In order to illustrate that the model is able to transition between states, we start a simulation with conditions characterizing one state, and at later time points switch to the parameter regime for another state.

Transition from healthy state to diseased state: To show a transition from healthy to diseased state, we begin with the parameter values and initial conditions for the healthy state, and at $t = 3000$ introduce parameter changes corresponding to the diseased state. As we see in Fig. 8, this leads to AA profile marked by very short growth stage.

Transition from diseased state to treatment state: To simulate transition from diseased to treatment state, we start with parameters and initial conditions set to their diseased state levels, and at $t = 3000$ we change the parameters to treatment state values. As Fig. 9 shows, the follicle exhibits short anagen phases up until $t = 3000$, and after that the growth stage is restored to its usual length.

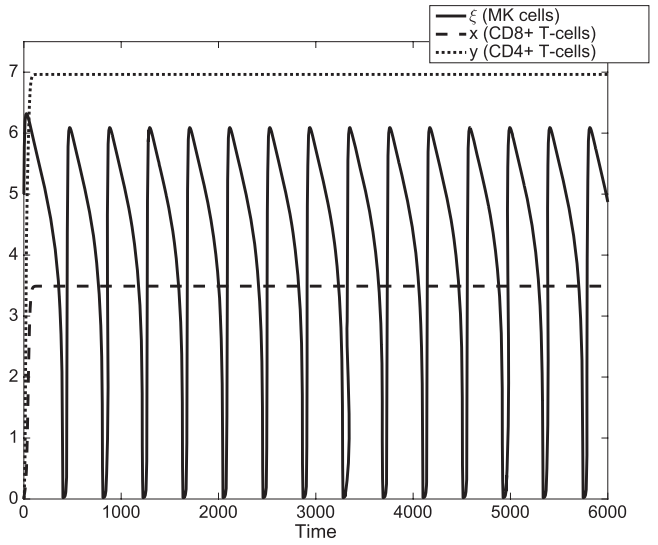

FIG. 6. Diseased state: Anagen with significantly shortened duration. Over time the lymphocyte populations reach high levels and cause disease.

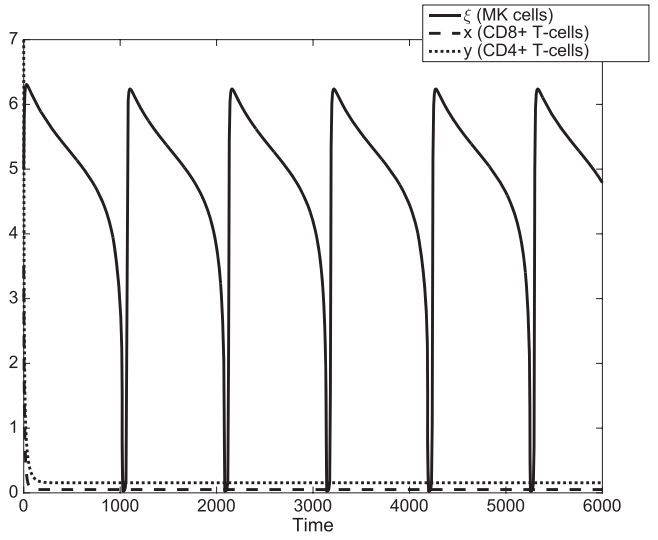

FIG. 7. Treatment state: Normal length of anagen recovered. Sufficiently high amount of potent HF IPG causes the lymphocyte populations to diminish to very low levels, and AA is suppressed.

Transition from healthy state to diseased state to treatment state: The model is also capable of transitions among all three scenarios (Fig. 10). We begin with the parameter values and initial conditions for the healthy state. At $t = 3000$, we make the parameter changes corresponding to the diseased state, which leads to AA development. Next, at $t = 4500$ we switch to the treatment state parameter regime, and the normal length of anagen is recovered.

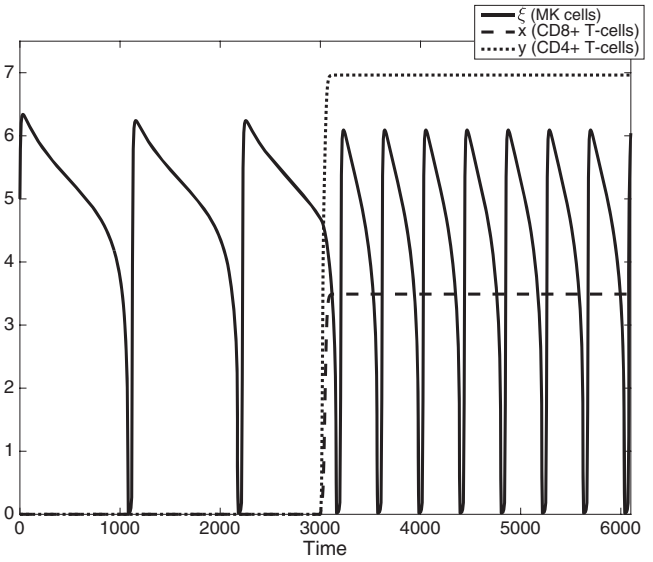

FIG. 8. Transition from healthy state to diseased state.

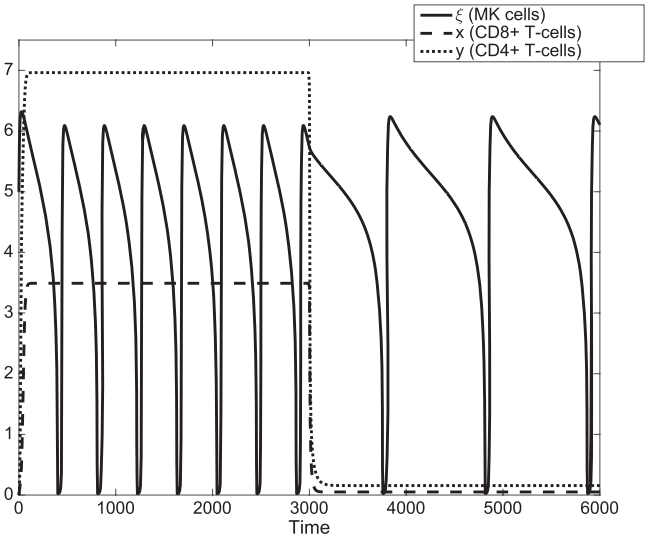

FIG. 9. Transition from diseased state to treatment state.

3.2 *Sensitivity analysis*

In this section we apply parameter sensitivity analysis to the hair cycle and composite models, and we compare the results in order to assess how different processes influence the duration of anagen in a healthy follicle and in a follicle diseased with AA. Sensitivity analysis entails varying the parameters in a model, simulating the system, gathering information on an outcome of interest, and computing sensitivity measures. The measures, depending on the method applied, are called coefficients or indices,

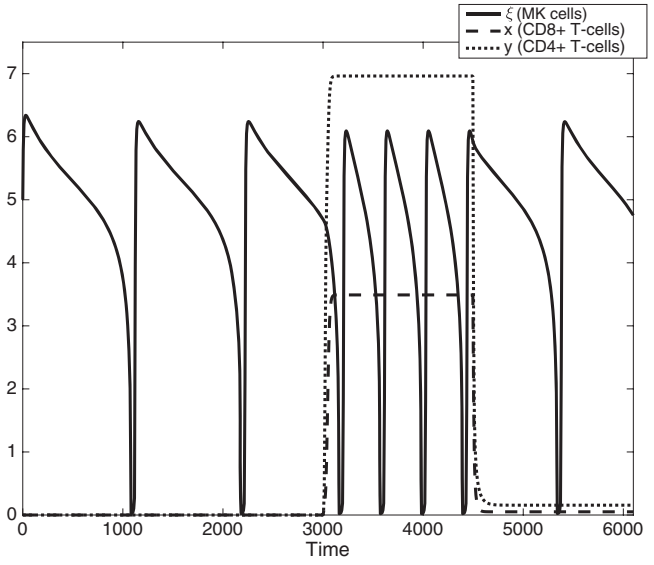

FIG. 10. Transition from healthy state to diseased state to treatment state.

and they show how variations in parameters influence changes in the desired output. In sensitivity analysis literature, parameters are also called input factors (Marino *et al.*, 2008).

For the models we analyse, the outcome we are interested in is the length of time that the MK level is under a specified low threshold value ($\xi = 0.1$). The reason is that when anagen has normal duration (on the order of two to five years), the amount of time that the population of MKs would be below threshold is significantly less compared to when the growth stage is very short (on the order of a few months or weeks).

We use the sensitivity analysis method referred to as Extended Fourier Amplitude Sensitivity Test (eFAST) which is capable of handling non-monotonic relationships between parameters (input factors) and the desired output (Marino *et al.*, 2008; Saltelli *et al.*, 1999, 2000). The method involves decomposing the variance in the desired outcome caused by variation in individual parameters or groups of parameters (Saltelli *et al.*, 2000, 2006). eFAST produces two quantitative measures, first order sensitivity index and total order sensitivity index. The first order sensitivity index shows the individual contribution of each parameter to the output variance. The total order sensitivity index measures how much a parameter contributes to the output variance individually as well as in interaction with other parameters. Parameter importance is determined by the magnitude of its corresponding sensitivity indices (Marino *et al.*, 2008; Saltelli *et al.*, 1999, 2000).

In the hair cycle model sensitivity analysis, we follow the standard procedure of varying all parameters, simulating the model and collecting outcome values, and calculating sensitivity indices for each parameter. On the other hand, the sensitivity analysis methodology we employ for the composite model involves grouping of parameters (Saltelli *et al.*, 2000, 2006) in order to account for the distinctive feature that MK apoptosis is impacted by autoreactive immune cells. The sequence of steps we perform is as follows:

(1) Group parameter p_4 with the parameters from the immune components sub-model (s, v, l, a, b, w). This group, which we label G, reflects the process of MK apoptosis under the influence of autoreactive immune cells.

TABLE 3 *Parameter ranges and baseline values used in eFAST sensitivity analysis*

Parameter	Range	Baseline value
s	[0.0003, 5.5]	0.00034
v	[0.11, 0.55]	0.32
l	[0.005, 1.25]	0.6319
a	[0.0002, 2.5]	2.381
b	[0.0005, 5.5]	0.000525
w	[0.055, 0.11]	0.0837
p_1	[0.45, 0.5]	0.48
p_2	[0.095, 0.11]	0.1
p_3	[0.095, 0.11]	0.1
p_4	[0.25, 0.56]	0.5
p_5	[0.225, 0.475]	0.32
C_{prol}	[0.9, 1.115]	0.1
α	[0.095, 0.11]	0.1
β	[0.005, 0.015]	0.1
k	[1.8, 2.05]	2.0385
c_1	[0.5, 1.125]	1
c_2	[0.5, 1.125]	1
D_η	[0.435, 0.75]	0.5
D_z	[0.095, 0.15]	0.1

(2) Sample parameters treating the group G as a single input factor.

(3) Simulate the composite model and obtain values for the outcome of interest.

(4) Compute sensitivity indices for the parameter group G and the remaining parameters in the hair cycle sub-model.

Due to insufficient information regarding the underlying distributions of parameters, we assume that the values of all parameters follow uniform distributions, which is a widely used strategy in such cases. The ranges over which parameters vary together with baseline values are given in Table 3.

The eFAST sensitivity analysis results for the hair cycle model, presented in Fig. 11, show that the parameters with highest first order and total order effects on the duration of anagen are p_4, β, k, c_1, c_2, D_η and D_z. These results indicate that in healthy HFs the processes fundamental for the growth phase length are MK apoptosis, MK population decrease due to factors other than apoptosis, feedforward inhibition of MK apoptosis, signalling molecule production and permeation and regulatory molecule production and permeation. Also, there is pronounced interaction among parameters in the model. (For parameter descriptions see Table 1.)

The eFAST analysis results for the composite model are shown in Fig. 12. As before, there are prominent parameter interactions. The parameters with strongest first order effects on the growth phase duration are G, p_1, p_2, k, c_1, c_2 and D_η. As explained earlier in this section, the group of parameters G reflects the process of MK apoptosis under the impact of autoreactive lymphocytes. So, the pronounced

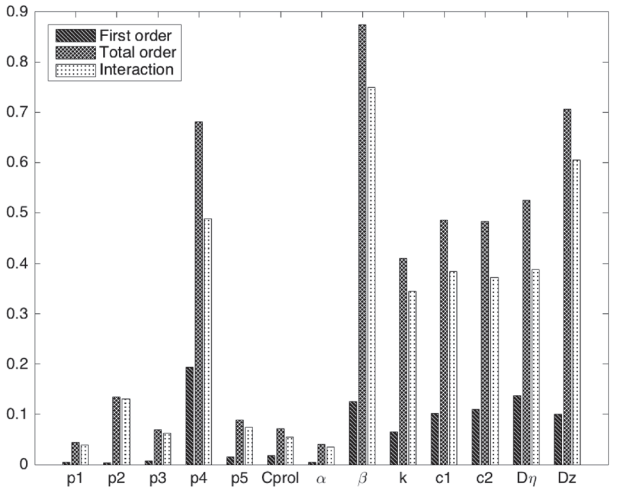

FIG. 11. eFAST sensitivity analysis results for hair cycle model with length of anagen phase as outcome of interest. The interaction index for each input factor is obtained by subtracting its first order sensitivity index from its total order sensitivity index.

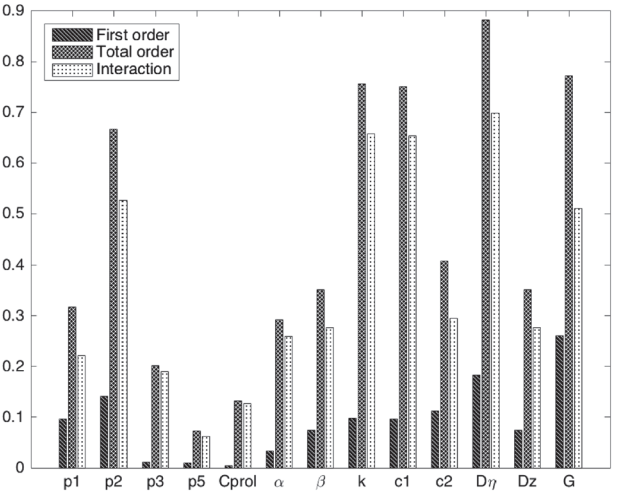

FIG. 12. eFAST sensitivity analysis results for composite model with length of anagen phase as outcome of interest. The interaction index for each input factor is obtained by subtracting its first order sensitivity index from its total order sensitivity index.

sensitivity with respect to G indicates that in HFs susceptible to AA, the length of anagen changes robustly in response to variations in the apoptosis rate. In addition, alterations in the proliferation of MKs as well as the half-saturation level for MK population increase lead to conspicuous changes in the growth phase duration. The parameters with highest total order effects are G, p_1, p_2, α, β, k, c_1, c_2, D_η and D_z. The noticeable sensitivity with respect to α suggests that in AA-affected HFs the process of stem cell input into the population of MKs plays a crucial role for how long anagen lasts.

Comparing the sets of results for the two models reveals that while p_1, p_2 and α are not identified as important in the hair cycle model, they gain significance in the composite model. While the first order effects of p_1 and p_2 become noticeably stronger in contrast to the hair cycle model, the increase in the first order effect of α is not as large. On the other hand, all three parameters exhibit significant increase in their interaction effects. In addition, in the composite model, k, c_1 and D_η have increased interaction effects, and consequently higher total effects. These results imply that, in relation to the duration of the growth phase, susceptibility to AA brings importance to the population increase processes of proliferation and stem cell input and makes stronger the influence of signalling molecule dynamics as well as feedforward inhibition of MK apoptosis. On the other hand, β, c_2 and D_z have lower total effects in the composite model primarily due to diminished interaction effects. This indicates that regulatory molecule dynamics and population decrease processes other than apoptosis become secondary factors in determining the length of anagen in HFs affected by AA.

4. Discussion

In this work we propose a way to connect in a composite dynamical system a previously established model for the hair cycle (Al-Nuaimi *et al.*, 2012) with a model that tracks the dynamics of immune system constituents involved in the development of AA (Dobreva *et al.*, 2015). Based on experimental studies, we incorporate a function which feeds the immune model output into the apoptosis term of the hair cycle system. Our composite model is able to qualitatively capture the behaviour of a small cluster of disease-affected cycling HFs. More specifically, the results demonstrate cycle interruption resulting from an autoimmune response against HFs.

In accordance with experimental and clinical evidence, the model predicts that high level of IFN-γ, which is a very strong catagen induction signal and promotes both HF dystrophy and HF IP collapse (Ito *et al.*, 2004, 2005), causes large accumulations of activated autoreactive $CD4^+$ and $CD8^+$ T-cells/$NKG2D^+$ cells. These, together with the cytotoxic effects of IFN-γ itself, inflict excessive, premature and ectopic apoptosis at an accelerated rate on MKs, leading to very short, aborted and dystrophic anagen phase. Our simulation results are also consistent with the recognized disease feature that while the growth phase duration gets affected, catagen and telogen retain largely normal length.

In addition, the composite model illustrates that introducing a large amount of strong IP guardians in diseased HFs diminishes the populations of autoreactive immune cells to very low levels. This in turn suppresses progression of AA and brings anagen back to its normal length. While this had previously been postulated on the basis of biological and clinical arguments alone (Paus *et al.*, 2005), we have now generated a mathematical model that permits one to accurately predict this chain of events, including how spontaneous or iatrogenic variations of individual parameters in this model affect the overall outcome. Furthermore, the model is capable of making transitions among the states of health, disease and treatment.

Applying parameter sensitivity analysis shows that the process of MK apoptosis has an essential role in relation to the growth stage length. Also, modulation of feedforward inhibition of MK apoptosis stands out as an influential factor for how long anagen lasts. This is well in line with what has previously been shown by the Al-Nuaimi *et al.* model that simulates the physiological control of anagen in healthy HFs (Al-Nuaimi *et al.*, 2012). Furthermore, the sensitivity analysis indicates that under the impact of autoreactive immune components, MK proliferation and stem cell input to the MK population gain significance in connection to the duration of anagen. On the other hand, loss of MKs due to processes other than apoptosis (e.g. terminal differentiation of MKs into fully keratinized hair shaft trichocytes (Thibaut *et al.*, 2005; Langbein & Schweizer, 2005; Purba *et al.*, 2016)) loses some of its impact. This last result could be associated with a clinical phenomenon in AA which concerns hair shape. There is

some evidence to suggest that hair shape is dictated in the hair matrix (Thibaut *et al.*, 2005). So, alterations in the rate and quality of MK differentiation into trichocytes during HF recovery from AA might actually explain why hair regrowth in some AA patients can go along with changes in hair shape.

Our results also indicate that signalling between MKs and DP cells plays a principal part in determining the growth phase duration, not only in healthy, but also in diseased HFs. In contrast, while in a healthy HF the dynamics of regulatory molecules have a crucial impact on the length of anagen, under influence of an autoaggressive inflammatory infiltrate that attacks the HF in AA, they seem to have a decreased effect. This may be related to the fact that IFN-γ, the chief cytokine driving AA pathobiology (Gilhar *et al.*, 2012; McElwee *et al.*, 2013), is also a much stronger catagen-promoting signal in human anagen HFs (at least *ex vivo*) than TGF-β1 and TGF-β2, the main catagen-inducing growth factors during the physiological anagen-catagen transformation (Paus and Foitzik , 2004; Ito *et al.*, 2005; Langan *et al.*, 2015).

While much ongoing pivotal work has explored and defined in ever more detail the contribution of individual molecular pathways, albeit predominantly in mice (Plikus *et al.*, 2008; Plikus, 2012; Geyfman *et al.*, 2014; Lien *et al.*, 2014; Kloepper *et al.*, 2014; Andl & Botchkareva, 2015; Sennett *et al.*, 2015; Fuchs, 2016; Widelitz & Chuong , 2016), it has not yet been comprehensively elucidated if and how signalling between MKs, DP cells and epithelial stem cells gets altered in human HFs affected by AA. Our sensitivity analysis findings suggest that this is an area worth investigating for the purpose of identifying new potential therapeutic targets.

The sensitivity analysis results also point to prominent interactions among processes in the composite model. In addition to acting as key guardians of HF IP (Paus *et al.*, 2005), TGF-β1 and TGF-β2 play an important role in the communication between hair producing cells and the DP (Stenn & Paus, 2001; Botchkarev and Kishimoto, 2003; Sennett & Rendl, 2012; Oshimori & Fuchs, 2012). This provides some explanation for the strong interaction effects we observe among processes in our composite model. The immune components sub-system reflects the suppressive activity of TGF-β toward autoreactive lymphocytes. This is why, it is plausible that in connecting this model to the hair cycle system, to account for the impact of immune cells, TGF-β comes to also factor in the MK-DP communication.

In this study we aimed to enhance the capabilities of our previously proposed model for the development of AA, which had shown that incorporating the IP collapse hypothesis for the disease pathogenesis (Paus *et al.*, 1993) into a modelling framework is able to capture the qualitative immunopathology observed in AA (Dobreva *et al.*, 2015). By coupling the immune system dynamics to the hair cycle, in the current study, we are working towards improving the predictive nature of the model.

Certainly, validation and further elaboration and refinement are necessary to attain predictive power. For example, other important, yet secondary immunocyte populations relevant to AA pathogenesis, such as mast cells, regulatory T-cells and NK cells, can be included in the model. In addition, validation can be achieved in part through using the composite dynamical system to represent some existing treatments for AA, such as glucocorticosteroids, contact sensitizers, cyclosporine A, or JAK inhibitors (Gilhar *et al.*, 2012; Iorizzo & Tosti, 2015; Jabbari *et al.*, 2015, 2016; Renert-Yuval & Guttman-Yassky, 2016; Tavakolpour *et al.*, 2016). For this purpose, one needs to outline parameter regimes and parameter perturbations that correspond to different therapeutic alternatives and capture the effects described in available clinical AA studies. Having a grip on that will also allow for using the model to test hypothetical treatment response scenarios which could hopefully provide some new results and insights relevant to biologists and clinicians investigating AA.

Moreover, accepting that the cycling HF provides an excellent general model system for computational and systems biology (Al-Nuaimi *et al.*, 2010) while AA represents a highly instructive general model for T cell-dependent autoimmune diseases characterized by cyclic change in their clinical course and phenotype

(Gilhar *et al.*, 2007, 2012), our current model has the potential to serve as a platform for probing how principles and tools of mathematical modelling, computational biology and sensitivity analysis can be applied to a human autoimmune disease in a translationally relevant manner.

Funding

This study was supported by the National Science Foundation (grant number: nsf math biology 1510743) and the NIHR Manchester Biomedical Research Centre ("Inflammatory Hair Diseases" Programme).

References

Alli, R., Nguyen, P., Boyd, K., Sundberg, J. P. & Geiger, T. L. (2012) A mouse model of clonal CD8+ T lymphocyte-mediated alopecia areata progressing to alopecia universalis. *J. Immunol.*, **188**, 477–486.

Al-Nuaimi, Y., Baier, G., Watson, R. E., Chuong, C. M. & Paus, R. (2010) The cycling hair follicle as an ideal systems biology research model, *Exp. Dermatol.*, **19**, 707–713.

Al-Nuaimi, Y., Goodfellow, M., Paus, R. & Baier, G. (2012) A prototypic mathematical model of the human hair cycle, *J. Theor. Biol.*, **310**, 143–159.

Andl, T. & Botchkareva, N. V. (2015) MicroRNAs (miRNAs) in the control of HF development and cycling: the next frontiers in hair research, *Exp. Dermatol.*, **24**, 821–826.

Baker, R. E. & Murray, P. J. (2012) Understanding hair follicle cycling: a systems approach, *Curr. Opin. Genet. Dev.*, **22**, 607–612.

Bernard, B. A. (2012) The human hair follicle, a bistable organ? *Exp. Dermatol.*, **21**, 401–403.

Bertolini, M., Pretzlaff, M., Sulk, M., Bähr, M., Gherardini, J., Uchida, Y., Reibelt, M., Kinori, M., Rossi, A., Bíró, T. & Paus, R. (2016) Vasoactive intestinal peptide, whose receptor-mediated signalling may be defective in alopecia areata, provides protection from hair follicle immune privilege collapse, *Br. J. Dermatol.*, **175**, 531–541.

Bertolini, M., Zilio, F., Rossi, A., Kleditzsch, P., Emelianov, V. E., Gilhar, A., Keren, A., Meyer, K. C., Wang, E., Funk, W., McElwee, K. & Paus, R. (2014) Abnormal interactions between perifollicular mast cells and $CD8^+$ T-cells may contribute to the pathogenesis of alopecia areata, *PLoS One*, **9**, e94260.

Botchkarev, V. A. & Kishimoto, J. (2003) Molecular control of epithelial-mesenchymal interactions during hair follicle cycling, *J. Investig. Dermatol. Symp. Proc.*, **8**, 46–55.

Dobreva, A., Paus, R. & Cogan, N. G. (2015) Mathematical model for alopecia areata, *J. Theor. Biol.*, **380**, 332–345.

D'Ovidio, R. (2014) Alopecia Areata: news on diagnosis, pathogenesis and treatment, *G. Ital. Dermatol. Venereol.*, **149**, 25–45.

Fuchs, E. (2016) Epithelial skin biology: three decades of developmental biology, a hundred questions answered and a thousand new ones to address, *Curr. Top. Dev. Biol.*, **116**, 357–374.

Geyfman, M., Kumar, V., Liu, Q., Ruiz, R., Gordon, W., Espitia, F., Cam, E., Millar, S. E., Smyth, P., Ihler, A., Takahashi, J. S. & Andersen, B. (2012) Brain and muscle Arnt-like protein-1 (BMAL1) controls circadian cell proliferation and susceptibility to UVB-induced DNA damage in the epidermis, *Proc. Natl. Acad. Sci. USA*, **109**, 11758–11763.

Geyfman, M., Plikus, M. V., Treffeisen, E., Andersen, B. & Paus, R. (2014) Resting no more: re-defining telogen, the maintenance stage of the hair growth cycle, *Biol. Rev. Camb. Philos. Soc.*, **90**, 1179–1196.

Gilhar, A., Etzioni, A. & Paus, R. (2012) Medical progress: alopecia areata, *N. Engl. J. Med.*, **366**, 1515–1525.

Gilhar, A., Keren, A., Shemer, A., d'Ovidio, R., Ullmann, Y. & Paus, R. (2013) Autoimmune disease induction in a healthy human organ: a humanized mouse model of alopecia areata, *J. Invest. Dermatol.*, **133**, 844–847.

Gilhar, A., Paus, R. & Kalish, R. S. (2007) Lymphocytes, neuropeptides, and genes involved in alopecia areata, *J. Clin. Invest.*, **117**, 2019–2027.

Gilhar, A., Schrum, A. G., Etzioni, A., Waldmanne, H. & Paus, R. (2016) Alopecia areata: animal models illuminate autoimmune pathogenesis and novel immunotherapeutic strategies, *Autoimmun. Rev.*, **15**, 726–735.

GILHAR, A., ULLMANN, Y., BERKUTZKI, T., ASSY, B. & KALISH, R. S. (1998) Autoimmune hair loss (alopecia areata) transferred by T lymphocytes to human scalp explants on SCID mice, *J. Clin. Invest.*, **101**, 62–67.

GUO, H., CHENG, Y., SHAPIRO, J. & MCELWEE, K. (2015) The role of lymphocytes in the development and treatment of alopecia areata, *Autoimmun. Rev.*, **11**, 1335–1351.

HALLE, S., KEYSER, K. A., STAHL, F. R., BUSCHE, A., MARQUARDT, A., ZHENG, X., GALLA, M., HEISSMEYER, V., HELLER, K., BOELTER, J., WAGNER, K., BISCHOFF, Y., MARTENS, R., BRAUN, A., WERTH, K., UVAROVSKII, A., KEMPF, H., MEYER-HERMANN, M., ARENS, R., KREMER, M., SUTTER, G., MESSERLE, M. & FÖRSTER, R. (2016) In vivo killing capacity of cytotoxic T cells is limited and involves dynamic interactions and T cell cooperativity, *Immunity*, **44**, 233–245.

HALLOY, J., BERNARD, B. A., LOUSSOUARN, G. & GOLDBETER, A. (2000) Modeling the dynamics of human hair cycles by a follicular automaton, *Proc. Natl. Acad. Sci. USA* , **97**, 8328–8333.

HALLOY, J., BERNARD, B. A., LOUSSOUARN, G. & GOLDBETER, A. (2002) The follicular automaton model: effect of stochasticity and of synchronization of hair cycles, *J. Theor. Biol.*, **214**, 469–479.

HARDMAN, J. A., TOBIN, D. J., HASLAM, I. S., FARJO, N., FARJO, B., AL-NUAIMI, Y., GRIMALDI, B., & PAUS, R. (2015) The peripheral clock regulates human pigmentation, *J. Invest. Dermatol.*, **135**, 1053–1064.

IORIZZO, M., & TOSTI, A. (2015) Treatments options for alopecia, *Expert. Opin. Pharmacother.*, **16**, 2343–2354.

ISLAM, N., LEUNG, P. S. C., HUNTLEY, A. C. & GERSHWIN, M. E. (2015) The autoimmune basis of alopecia areata: A comprehensive review, *Autoimmun. Rev.*, **14**, 81–89.

ITO, T. (2013) Recent advances in the pathogenesis of autoimmune hair loss disease alopecia areata, *Clin. Dev. Immunol.*, **2013**, 1–6.

ITO, T., ITO, N., BETTERMANN, A., TOKURA, Y., TAKIGAWA, M. & PAUS, R. (2004) Collapse and restoration of MHC Class-I-dependent immune privilege, *Am. J. Pathol.*, **164**, 623–634.

ITO, T., ITO, N., SAATHOFF, M., BETTERMANN, A., TAKIGAWA, M. & PAUS, R. (2005) Interferon-gamma is a potent inducer of catagen-like changes in cultured human anagen hair follicles, *Br. J. Dermatol.*, **152**, 623–631.

ITO, T., ITO, N., SAATOFF, M., HASHIZUME, H., FUKAMIZU, H., NICKOLOFF, B., TAKIGAWA, M. & PAUS, R. (2008) Maintenance of hair follicle immune privilege is linked to prevention of NK cell attack, *J. Invest. Dermatol.*, **128**, 1196–1206.

ITO, T. & TOKURA, Y. (2014) The role of cytokines and chemokines in the T-cell-mediated autoimmune process in alopecia areata, *Exp. Dermatol.*, **23**, 787–791.

JABBARI, A., DAI, Z., XING, L., CERISE, J. E., RAMOT, Y., BERKUN, Y., SANCHEZ, G. A., GOLDBACH-MANSKY, R., CHRISTIANO, A. M., CLYNES, R. & ZLOTOGORSKI, A. (2015) Reversal of alopecia areata following treatment with the JAK1/2 inhibitor baricitinib, *EBioMedicine*, **2**, 351–355.

JABBARI, A., NGUYEN, N., CERISE, J. E., ULERIO, G., DE JONG, A., CLYNES, R., CHRISTIANO, A. M. & MACKAY-WIGGAN, J. (2016) Treatment of an alopecia areata patient with tofacitinib results in regrowth of hair and changes in serum and skin biomarkers, *Exp. Dermatol.*, **25**, 642–643.

KINORI, M., BERTOLINI, M., FUNK, W., SAMUELOV, L., MEYER, K. C., EMELIANOV, V. U., HASSE, S. & PAUS, R. (2012) Calcitonin gene-related peptide (CGRP) may award relative protection from interferon-Î³induced collapse of human hair follicle immune privilege, *Exp. Dermatol.*, **21**, 223–226.

KLOEPPER, J. E., ERNST, N., KRIEGER, K., BODÓ, E., BÍRÓ, T., HASLAM, I. S., SCHMIDT-ULLRICH, R. & PAUS, R. (2014) NF-κB activity is required for anagen maintenance in human hair follicles *in vitro*, *J. Invest. Dermatol.*, **134**, 2036–2038.

LANGAN, E. A., PHILPOTT, M. P., KLOEPPER, J. E. & PAUS, R. (2015) Human hair follicle organ culture: theory, application and perspectives, *Exp. Dermatol.*, **24**, 903–911.

LANGBEIN, L. & SCHWEIZER, J. (2005) Keratins of the human hair follicle, *Int. Rev. Cytol.*, **243**, 1–78.

LIEN, W. H., POLAK, L., LIN, M., LAY, K., ZHENG, D. & FUCHS, E. (2014) *In vivo* transcriptional governance of hair follicle stem cells by canonical Wnt regulators, *Nat. Cell. Biol.*, **16**, 179–190.

MARINO, S., HOGUE, I. B., RAY, C. J. & KIRSCHNER, D. E. (2008) A methodology for performing global uncertainty and sensitivity analysis in systems biology, *J. Theoret. Biol.*, **254**, 178–196.

MCDONAGH, A. J. & MESSENGER, A. G. (2001) Alopecia areata, *Clin. Dermatol.*, **19**, 141–147.

McElwee, K. J., Gilhar, A., Tobin, D. J., Ramot, Y., Sundberg, J. P., Nakamura, M., Bertolini, M., Inui, S., Tokura, Y., King Jr., L. E., Duque-Estrada, B., Tosti, A., Keren, A., Itami, S., Shoenfeld, Y., Zlotogorski, A. & Paus, R. (2013) What causes alopecia areata? *Exp. Dermatol.*, **22**, 609–626.

Morgan, B. A. (2014) The dermal papilla: an instructive niche for epithelial stem and progenitor cells in development and regeneration of the hair follicle, *Cold Spring Harb. Perspect. Med.*, **4**, a015180.

Murray, P. J., Maini, P. K., Plikus, M. V., Chuong, C. M., & Baker, R. E. (2012) Modelling hair follicle growth dynamics as an excitable medium, *PLoS Comput. Biol.*, **8**, e1002804.

Oh, J. W., Kloepper, J., Langan, E. A., Kim, Y., Yeo, J., Kim, M. J., Hsi, T. C., Rose, C., Yoon, G. S., Lee, S. J., Seykora, J., Kim, J. C., Sung, Y. K., Kim, M., Paus, R. & Plikus, M. V. (2016) A guide to studying human hair follicle cycling in vivo, *J. Invest. Dermatol.*, **136**, 34–44.

Ohyama, M., Zheng, Y., Paus, R. & Stenn, K. S. (2010) The mesenchymal component of hair follicle neogenesis: background, methods and molecular characterization, *Exp. Dermatol.*, **19**, 89–99.

Oshimori, N. & Fuchs, E. (2012) Paracrine TGF-β signaling counterbalances BMP-mediated repression in hair follicle stem cell activation, *Cell Stem Cell*, **10**, 63–75.

Paus, R., Arck, P. & Tiedea, S. (2008) (Neuro-)endocrinology of epithelial hair follicle stem cells, *Mol. Cell. Endocrinol.*, **288**, 38–51.

Paus, R. & Foitzik, K. (2004) In search of the "hair cycle clock": a guided tour, *Differentiation*, **72**, 489–511.

Paus, R., Nickoloff, B. J. & Ito, T. (2005) A 'hairy' privilege, *Trends Immunol.*, **26**, 32–40.

Paus, R., Slominski, A. & Czametzki, B. M. (1993) Is alopecia areata an autoimmune-response against melanogenesis-related proteins, exposed by abnormal MHC class I expression in the anagen hair bulb? *Yale J. Biol. Med.*, **66**, 541–554.

Petukhova, L., Duvic, M., Hordinsky, M., Norris, D., Price, V., Shimomura, Y., Kim, H., Singh, P., Lee, A., Chen, W., Meyer, K., Paus, R., Jahoda, C., Amos, C., Gregersen, P. & Christiano, A. (2010) Genome-wide association study in alopecia areata implicates both innate and adaptive immunity, *Nature*, **466**, 113–117.

Pevzner, P. (2000) *Computational Molecular Biology — An Algorithmic Approach*. Cambridge, MA: The MIT Press.

Plikus, M. V. (2012) New activators and inhibitors in the hair cycle clock: targeting stem cells' state of competence, *J. Invest. Dermatol.*, **132**, 1321–1324.

Plikus, M.V., Baker, R. E., Chen, C. C., Fare, C., de la Cruz, D., Andl, T., Maini, P. K., Millar, S. E., Widelitz, R. & Chuong, C. M. (2011) Self-organizing and stochastic behaviors during the regeneration of hair stem cells, *Science*, **332**, 586–589.

Plikus, M. V., Mayer, J. A., de la Cruz, D., Baker, R. E., Maini, P. K., Maxson, R. & Chuong, C. M. (2008) Cyclic dermal BMP signalling regulates stem cell activation during hair regeneration, *Nature*, **451**, 340–344.

Purba, T. S., Brunken, L., Hawkshaw, N. J., Peake, M., Hardman, J. & Paus, R. (2016) A primer for studying cell cycle dynamics of the human hair follicle, *Exp. Dermatol.*, **25**, 663–668.

Renert-Yuval, Y. & Guttman-Yassky, E. (2016) A novel therapeutic paradigm for patients with extensive alopecia areata, *Expert. Opin. Biol. Ther.*, **16**, 1005–10014.

Rose, N. R. & Mackay, I. (eds) (2013) *The Autoimmune Diseases*, 5th edn. New York, NY: Academic Press.

Saltelli, A., Tarantola, S. & Chan, K. P.-S. (1999) A quantitative model-independent method for global sensitivity analysis of model output, *Technometrics*, **41**, 39–56.

Saltelli, A., Tarantola, S. & Campolongo, F. (2000) Sensitivity analysis as an ingredient of modeling, *Stat. Sci.*, **15**, 377–395.

Saltelli, A., Ratto, M., Tarantola, S. & Campolongo, F. (2006) Sensitivity analysis practices: Strategies for model-based inference, *Reliab. Eng. Syst. Safe.*, **91**, 1109–1125.

Sennett, R. & Rendl, M. (2012) Mesenchymal-epithelial interactions during hair follicle morphogenesis and cycling, *Semin. Cell Dev. Biol*., **23**, 917–927.

Sennett, R., Wang, Z., Rezza, A., Grisanti, L., Roitershtein, N., Sicchio, C., Mok, K. W., Heitman, N. J., Clavel, C., Ma'ayan, A. & Rendl, M. (2015) An integrated transcriptome atlas of embryonic hair follicle progenitors, their niche, and the developing skin, *Dev. Cell*, **34**, 577–591.

SCHNEIDER, M. R., SCHMIDT-ULLRICH, R. & PAUS, R. (2009) The hair follicle as a dynamic miniorgan, *Curr. Biol.*, **19**, R132–R142.

STENN, K. S. & PAUS, R. (2001) Controls of hair follicle cycling, *Physiol. Rev.*, **81**, 449–494.

TAVAKOLPOUR, S., MAHMOUDI, H. R., DANESHPAZHOOH, M. & RAHIMZADEH, G. (2016) Complex interaction between diphenylcyclopropenone and immune responses in alopecia areata, *Scand. J. Immunol.*, **84**, 310–311.

THIBAUT, S., GAILLARD, O., BOUHANNA, P., CANNELL, D. W. & BERNARD, B. A. (2005) Human hair shape is programmed from the bulb, *Br. J. Dermatol.*, **152**, 632–638.

VAN SCOTT, E. J. & EKEL, T. M. PAUS, R. (1958) Geometric relationships between the matrix of the hair bulb and its dermal papilla in normal and alopecic scalp, *J. Invest. Dermatol.*, **31**, 281–287.

WATERMAN, M. S. (1995) *Introduction to Computational Biology: Maps, Sequences, Genomes*, 1st edn. Boca Raton, FL: Chapman & Hall/CRC Interdisciplinary Statistics.

WESTERHOFF, H. V. (2007) Systems biology: new paradigms for cell biology and drug design, *Ernst Schering Res. Found. Workshop*, **61**, 45–67.

WESTERHOFF, H. V., WINDER, C., MESSIHA, H., SIMEONIDIS, E., ADAMCZYK, M., VERMA, M., BRUGGEMAN, F. J. & DUNN, W. (2007) Systems biology: the elements and principles of life, *FEBS Lett.*, **583**, 3882–3890.

WESTERHOFF, H. V., NAKAYAMA, S., MONDEEL, T. D. & BARBERIS, M. (2015) Systems pharmacology: an opinion on how to turn the impossible into grand challenges, *Drug Discov. Today Technol.*, **15**, 23–31.

WIDELITZ, R. & CHUONG, C. M. (2016) Quorum sensing and other collective regenerative behavior in organ populations, *Curr. Opin. Genet. Dev.*, **40**, 138–143.

XING, L., DAI, Z., JABBARI, A., CERISE, J. E., HIGGINS, C. A., GONG, W., DEJONG, A., HAREL, S., DESTEFANO, G. M., ROTHMAN, L., SINGH, P., PETUKHOVA, L., MACKAY-WIGGAN, J., CHRISTIANO, A. M. & CLYNES, R. (2014) Alopecia areata is driven by cytotoxic T lymphocytes and is reversed by JAK inhibition, *Nat. Med.*, **20**, 1043–1049.